Zeitschrift: Schweizerische mineralogische und petrographische Mitteilungen = Bulletin suisse de minéralogie et pétrographie

Band: 62 (1982)

Heft: 1

Artikel: On physical and chemical properties of ruby muscovite used in the electrical industry

Autor: Klein, H.H. / Stern, W.B. / Weber, W.

DOI: https://doi.org/10.5169/seals-47967

Schweiz. mineral. petrogr. Mitt. 62, 145–173, 1982

On Physical and Chemical Properties of Ruby Muscovite used in the Electrical Industry

by *H. H. Klein* [1], *W. B. Stern* [2] and *W. Weber* [1]

Abstract

Ruby muscovites, from India (Bihar, Madras, Rajasthan), Morocco and Sudan have been studied by means of thermal techniques, X-ray diffraction, infrared- and X-ray spectrometry. According to grain size distribution the physical properties change significantly: fractions below 25 µm lose their endothermic DTA-peak near 850 °C, while a distinct trend towards higher peak temperatures for finer size fractions exists. X-ray experiments carried out on tempered single crystals show a drastic change of the lattice parameter c between 800 and 900 °C; i.e. the low temperature cell with $c \sim 19.94$ Å disappears above 800 °C, whereas a high temperature cell develops with $c \sim 20.1$ Å.

The hitherto reported provenience-specific IR absorption band at 3040 cm^{-1} (so called Bihar peak) is found in samples from several other origins, its interpretation as an ammonium frequency band has not been confirmed.

Wavelength-dispersive and energy-dispersive X-ray fluorescence analyses of 22 ruby micas show in certain cases a correlation of mica chemistry and mica provenience as far as phengitic components (iron and magnesium in octahedral sites) are considered.

Introduction

The combination of perfect cleavage, elasticity, low thermal conductivity and high dielectric strength makes muscovite an unique mineral. Best qualities of muscovite used in the electrical industry are only to be found in pegmatites.

The application of muscovite as an electrical insulating material (e.g. insulation of the conductor in rotating machines) requires a transformation of the mined mica into splittings or reconstituted mica paper. The labor intense, and therefore costly, manufacturing of mica splittings and its different, consecutive means of application have forced a distinct trend towards the development of mica paper in recent time.

Two different methods for manufacturing mica paper are known: either based on calcined mica (muscovite, treated at 700–800°) or uncalcined mica

[1] The Swiss insulating works, CH-4226 Breitenbach.

[2] Geochemical Labs/Mineralogical Institute, Basle University, CH-4056 Basel.

(muscovite and phlogopite). Calcined muscovite is easily disintegrated by means of a pulper, classified and transformed into paper by a horizontal paper machine [SKOW, (1962), US-Pat. 2549880 (BARDET, 1945)], whereas uncalcined mica is disintegrated by high pressure water jets [SKOW, (1962), US-Pat. 2405576 (HEYMAN, 1943)]. The mica flakes are only held together by their surface attraction.

According to the above mentioned method, mica papers display distinct properties: high tensile strength, high dielectric strength and poor porosity for mica papers based on calcined muscovite; poor tensile strength, poor dielectric strength and high porosity for mica papers based on uncalcined muscovite. The paper properties are furthermore influenced by the origin of mica, the grade of tectonical influences, its chemical composition, its purity, its freshness (no alteration products), its mining technique, etc. As recent and comprehensive data are lacking except in the case of certain Indian muscovites [DATTA, A.K. (1973)], the scope of this paper is essentially limited to the description of physical and chemical properties of muscovites used in the electrical industry.

By a combination of different analytical methods new data on muscovites of various origins have been compiled. The origin and literary sources of the reference is given in Tab. 1.

Ruby mica from the mentioned 5 proveniences have been industrially transformed into mica paper in order to check their ability and properties. Phlogo-

Tab. 1 Literary references: 1: DUNN, J.A. (1961), 2: DATTA, A.K. (1973), 3: MAHADEVAN, T.M. et al. (1961), 4: CHOUBERT, G. (1960), 5: BOULADON, J. et al. (1950), 6: KABESH, M.L. (1960), 7: Un-Report (1972).
Only literary references giving technical details of accurate data acquisition have been taken into consideration.

Reference	Country	State	Mine	Literature
A-1	India	Bihar	Saphi (Goenka)	1, 3
A-2	India	Bihar	Khirkia	1, 3
A-3	India	Bihar	Jhabra	1, 3
B	India	Madras	Sitarama, Gudur	1, 3
C-1	India	Rajasthan	Godas	1, 2
C-2	India	Rajasthan	Kuwanthal	1, 2
D	Morocco	Ouarzazate	Zenaga Pt.3	4, 5
E-1	Sudan	Nile Province	Abaza	6, 7
E-2	Sudan	Nile Province	Shilling Mica Area	6, 7
E-3	Sudan	Nile Province	Sudanese Mining Corp.	6, 7

pites and ruby micas from Brazil and Argentina have been examined, but any results are deliberately excluded from this paper due to the lack of in-depth field studies.

Thermal analysis

Dry ground muscovite samples were tested with a thermobalance (Mettler TA 2, see appendix). Fig. 1 shows the continuous weight loss between 200 and 1200 °C for samples with different grinding times. The total amount of weight loss has been normalized to 100%.

The effect of a creeping weight loss is increased by an extended milling time (BISHUI et al., 1961, PARKERT et al., 1950, MACKENZIE et al., 1953). The total amount at the loss on ignition increases (Fig. 3) and, furthermore, the endothermic DTA-area at approx. 850 °C due to the release of the OH-groups decreases.

A possible explanation for this uncommon behaviour might be found in the grain size distribution. The standardized sample preparation includes a washing process in ethanol. The washed mica is split up into pieces of approx. 0.5 mm thickness, a uniform size distribution of 5 x 5 mm pieces is obtained by manual scissor cutting. 10 resp. 30 g of the samples are fed to a laboratory disc mill (Retsch). The grinding elements of the mill are lined with WIDIA (W_2C, Co). The crushed sample is passed for 10 minutes through a bank of standard ASTM-sieves (HUTCHISON, 1974). The fraction 25 µm of five samples has been analysed by means of a Coulter Counter (see Fig. 2).

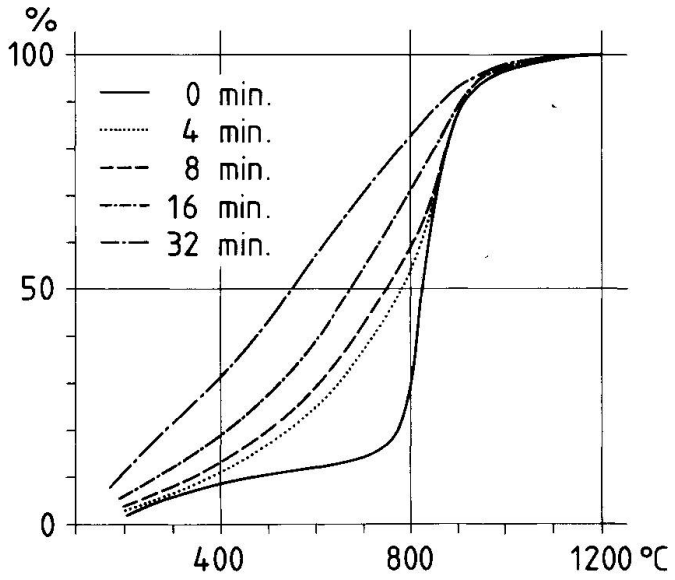

Fig. 1 Weight loss of muscovite A-1 (%) between 200 and 1200 °C as a function of mica grinding time, dynamic TG 10 °C/min.

Tab. 2 Grain size distribution of muscovite reference A-1 in function of the grinding time. The amount of the cumulative percentage of approx. 90% of the fraction < 25 µm is due to losses of the finest particles during draining.

Milling time	>250	>125	>63	>40	>25	<25 µm
4'	11	28	46	51	63	89
8'	7	23	40	46	58	92
16'	1	4	11	18	31	89
32'	< 1	2	9	16	30	90

The corresponding analysis shows - as expected - a higher amount of fine particles in function of the grinding time.

A second test series examines the grain size distribution of different muscovite samples (grinding time: 8 minutes).

Tab. 3 Grain size distribution in function of the origin.

Reference	>250	>125	>63	>40	>25	<25 µm
A - 1	7	23	40	46	58	92
C - 1	2	15	35	41	54	92
C - 2	4	17	35	42	55	90
E - 1	3	18	37	44	56	93
E - 2	1	10	27	35	50	94

Muscovite E-2 compared to the other samples represents a much harder mica.

The different sieve fractions are examined for their thermogravimetric behaviour.

The weight loss between 110 °C and 1100 °C is listed in Tab. 4; see Fig. 3.

The fine-grained fractions generally have a higher loss on ignition compared to coarse-grained fractions (see Fig. 3, Fig. 8). The difference of the weight loss is in the range of 20% relative and remains up to a temperature of 1600 °C (melting point of muscovite). The difference in weight loss is explained by a partial release of the alkalies; X-ray fluorescence investigations on a 1300 °C tempered sample showed the corresponding deficiency in alkalies (a loss of 1.3% K_2O i.e. ~ 10% rel. of the total potassium content of sample A-1).

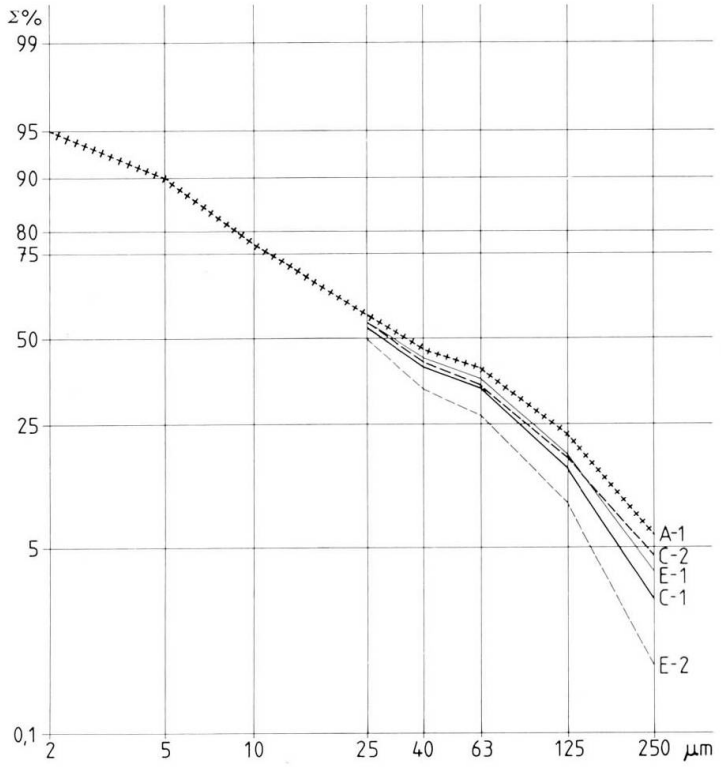

Fig. 2 Cumulative grain size distribution of the examined mica samples. The Coulter Counter analysis (model TA II) of the < 25 µm fraction by Plast Labor SA, 1630 Bulle/Switzerland, is gratefully acknowledged.

Fig. 3 Weight loss between 110 °C and 1100 °C for the selected grain size fraction (sample reference A-1), dynamic TG, 10 °C/min.

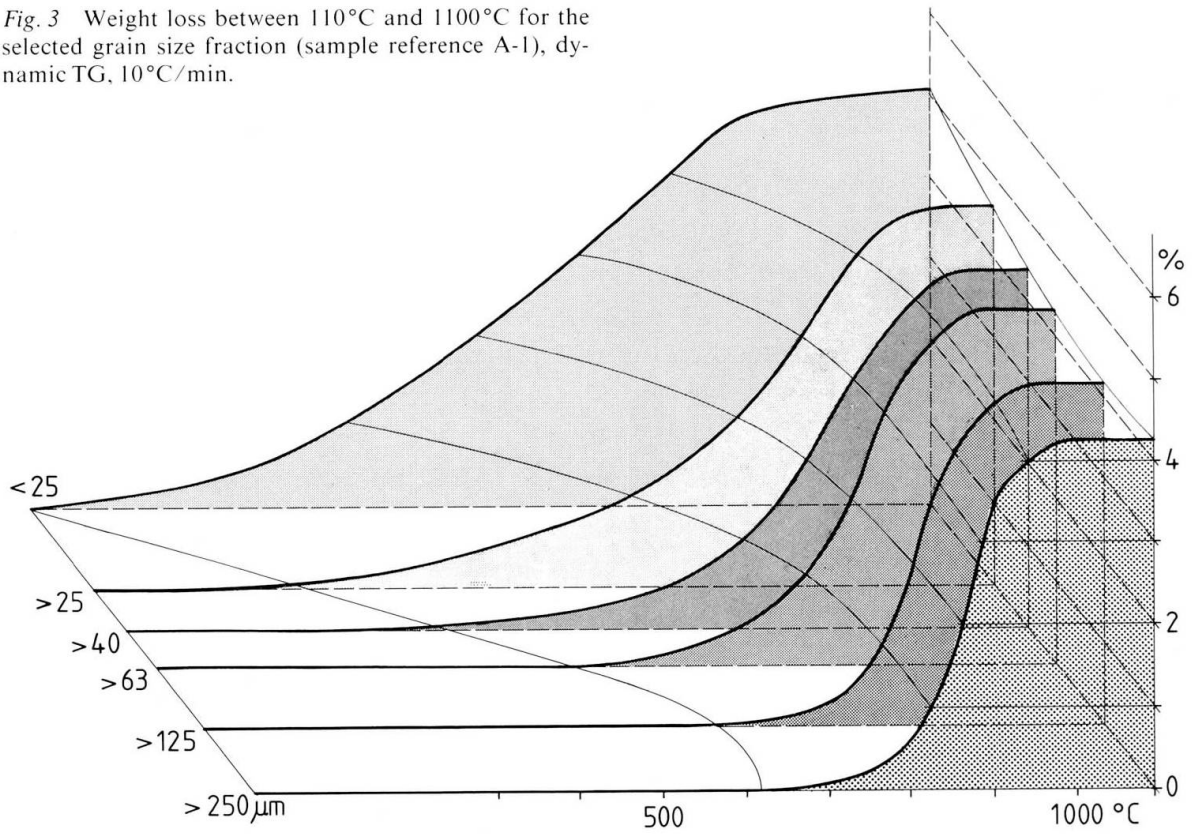

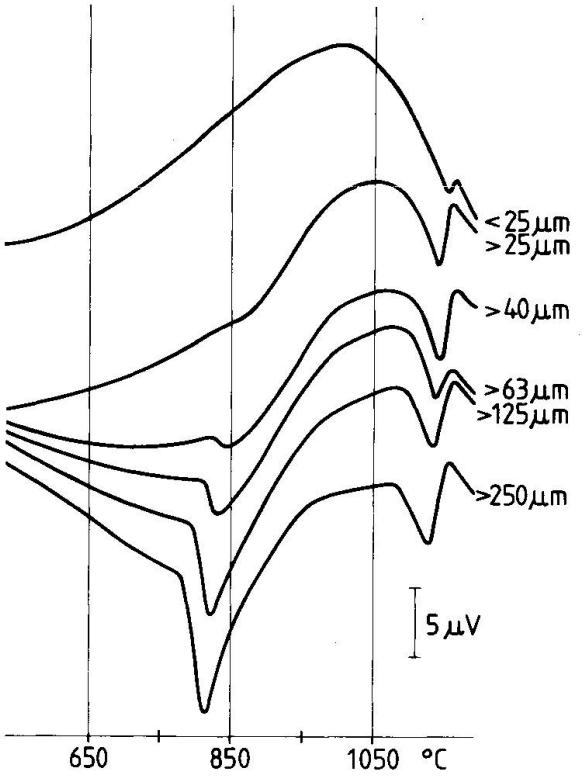

Fig. 4 DTA-graph vs. grain size of muscovite A-1.

Fig. 4 shows the DTA-curves for one sample (reference A-1) with different size distributions between < 25 µm and > 250 µm (for technical data see appendix).

The numeric interpretation is rather difficult due to a varying base line and a small peak area for the fine fractions. The calculation of the heat of reaction is based on the peak area, which is compared to silver (melting point: 961.3 °C) as a reference material.

Tab. 5 indicates the numeric value of the heat of reaction, ΔH_1 at approx. 850°, ΔH_2 at 1150 °C, T_1: starting temperature of the reaction [extrapolated, onset according to LOMBARDI, G. (1977)] and T_2: the apex temperature ΔH_1 is related to the release of the OH-groups and strongly dependent on the grain size, whereas ΔH_2 is probably correlated to the decomposition of muscovite [ROY (1949), YODER et al. (1955), VELDE, B. (1966)].

The temperature of the beginning and the apex of the reaction decreases with increasing grain size, whereas the heat of reaction increases. According to SCHULTZE (1969) the thermal decomposition takes place on the surface of the individual particles; therefore, the reaction is accelerated with decreasing particle size respectively starts at lower temperatures, contradictory to the above mentioned observations.

Tab. 4 Weight loss between 300 and 1100 °C in function of the grain size distribution.

Reference	Ø um	300 °C	400 °C	500 °C	600 °C	700 °C	800 °C	900 °C	1000 °C	1100 °C
A - 1	< 25	0.6	1.1	1.7	2.5	3.3	4.2	4.8	4.9	5.0
	> 25	0.1	0.3	0.5	0.8	1.3	2.1	3.6	4.5	4.6
	> 40	0.0	0.1	0.3	0.4	0.7	1.5	3.2	4.3	4.3
	> 63	0.0	0.0	0.1	0.1	0.4	1.1	3.2	4.3	4.3
	> 125	0.0	0.0	0.0	0.0	0.1	0.5	3.1	4.1	4.1
	> 250	0.0	0.0	0.0	0.0	0.1	0.5	3.4	4.2	4.2
C - 1	< 25	0.6	1.0	1.6	2.4	3.3	4.2	4.8	4.9	5.0
	> 25	0.1	0.3	0.5	0.7	1.2	2.2	3.7	4.5	4.5
	> 40	0.0	0.1	0.2	0.3	0.7	1.6	3.4	4.3	4.3
	> 63	0.0	0.0	0.1	0.2	0.5	1.3	3.3	4.3	4.4
	> 125	0.0	0.0	0.0	0.0	0.2	0.8	3.2	4.2	4.2
	> 250	0.0	0.0	0.0	0.0	0.1	0.6	3.3	4.2	4.2
C - 2	< 25	0.6	1.1	1.7	2.4	3.2	4.1	4.7	4.8	4.9
	> 25	0.1	0.3	0.5	0.7	1.2	2.0	3.3	4.3	4.3
	> 40	0.0	0.2	0.3	0.5	0.8	1.5	3.1	4.3	4.4
	> 63	0.0	0.0	0.0	0.1	0.4	1.0	2.7	4.1	4.2
	> 125	0.0	0.0	0.0	0.0	0.1	0.6	2.6	4.0	4.0
	> 250	0.0	0.0	0.0	0.0	0.1	0.5	3.0	4.1	4.2
E - 1	< 25	0.6	1.0	1.6	2.3	3.2	4.2	4.8	4.9	5.0
	> 25	0.1	0.2	0.3	0.5	0.9	1.8	3.2	4.2	4.2
	> 40	0.0	0.0	0.1	0.3	0.6	1.4	3.1	4.2	4.3
	> 63	0.0	0.0	0.0	0.1	0.4	1.0	3.0	4.3	4.3
	> 125	0.0	0.0	0.0	0.0	0.2	0.7	2.9	4.1	4.1
	> 250	0.0	0.0	0.0	0.0	0.1	0.5	3.2	4.2	4.2
E - 2	< 25	0.5	0.9	1.4	2.1	3.1	4.1	4.7	4.9	5.1
	> 25	0.0	0.2	0.3	0.5	1.0	2.0	3.3	4.1	4.2
	> 40	0.0	0.1	0.2	0.3	0.7	1.5	3.1	4.2	4.3
	> 63	0.0	0.0	0.0	0.1	0.3	1.0	2.8	4.0	4.1
	> 125	0.0	0.0	0.0	0.1	0.3	0.9	3.0	4.3	4.5
	> 250	0.0	0.1	0.1	0.2	0.4	0.9	3.4	4.4	4.6

Tab. 5 Calculated heat of reaction

Reference	grain size	reaction at appr.850°C			at appr.1150°C
	Ø	ΔH_1	T_1	T_2	ΔH_2
	(µm)	(J/g)	(°C)	(°C)	(J/g)
A - 1	< 25	< 5	---	---	32
	> 25	44	844	---	51
	> 40	74	840	853	55
	> 63	106	829	850	60
	> 125	120	820	843	57
	> 250	186	814	841	64
C - 1	< 25	< 5	---	---	16
	> 25	46	846	868	45
	> 40	82	836	859	57
	> 63	115	829	853	53
	> 125	158	826	841	51
	> 250	178	812	841	41
C - 2	< 25	< 5	---	---	30
	> 25	< 5	---	---	52
	> 40	75	839	---	65
	> 63	94	829	---	65
	> 125	137	818	852	50
	> 250	164	806	851	50
E - 1	< 25	< 5	---	---	33
	> 25	38	857	875	65
	> 40	61	852	873	63
	> 63	108	845	860	63
	> 125	138	842	855	62
	> 250	153	841	851	53
E - 2	< 25	< 5	---	---	37
	> 25	< 5	---	---	72
	> 40	53	839	864	67
	> 63	88	833	858	65
	> 125	131	822	857	63
	> 250	186	820	844	60

On the assumption that the heat of reaction of the > 250 µm fraction represents the asymptotic value, the heat of reaction varies between 153 and 186 J/g. The difference between the single values of the different muscovite samples lies probably in the range of error (see Tab. 5 and Fig. 5).

The decreasing endothermic peak area with decreasing particle size suggests a fractional deterioration of the lattice. The absence of the endothermic peak at approx. 850 °C of the mica particles less than 25 microns as well as the creeping weight loss shows the partial release of the OH-groups before the normally reported dehydration temperature. X-ray diffraction analyses, however, show that the examined lattice parameters do not change in function to grain size as

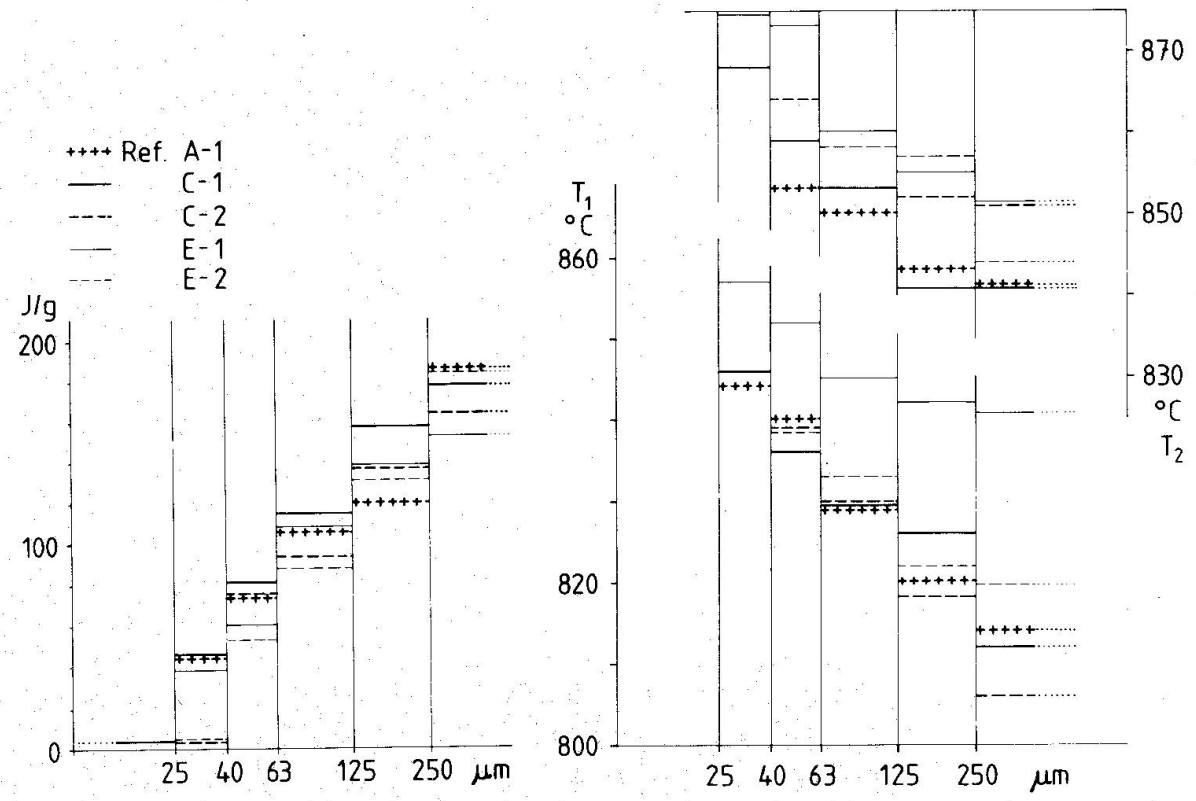

Fig. 5 Grain size versus heat of reaction rsp. temperature of dehydration of muscovites of different origins.

intensities of basal reflexions do (Fig. 6a, b). This could lead to the assumption of a disordered surface fraction. The expression "disordered" is not used in a strict crystallographic sense but could rather be interpreted as a partially destroyed/streched surface fraction of a crystal, thus enabling enhanced mobility of volatile components. Tab. 6 indicates the mean value of the disordered surface volume and the intact volume normalized to 100% of the endothermic peak area at approx. 850 °C (ΔH_1) in function of the grain size.

Tab. 6 Grain size distribution versus dehydration peak area and disordered volume based on experiments.

grain size (µm Ø)	disordered volume	intact volume	ΔH_1 - peak area (%) A-1	C-1	C-2	E-1	E-2
< 25	96%	4%	4	4	4	4	4
> 25	75%	25%	24	26	4	25	4
> 40	60%	40%	40	46	46	40	28
> 63	41%	59%	57	64	57	71	47
>125	21%	79%	64	88	83	91	70
>250	0	100%	100	100	100	100	100

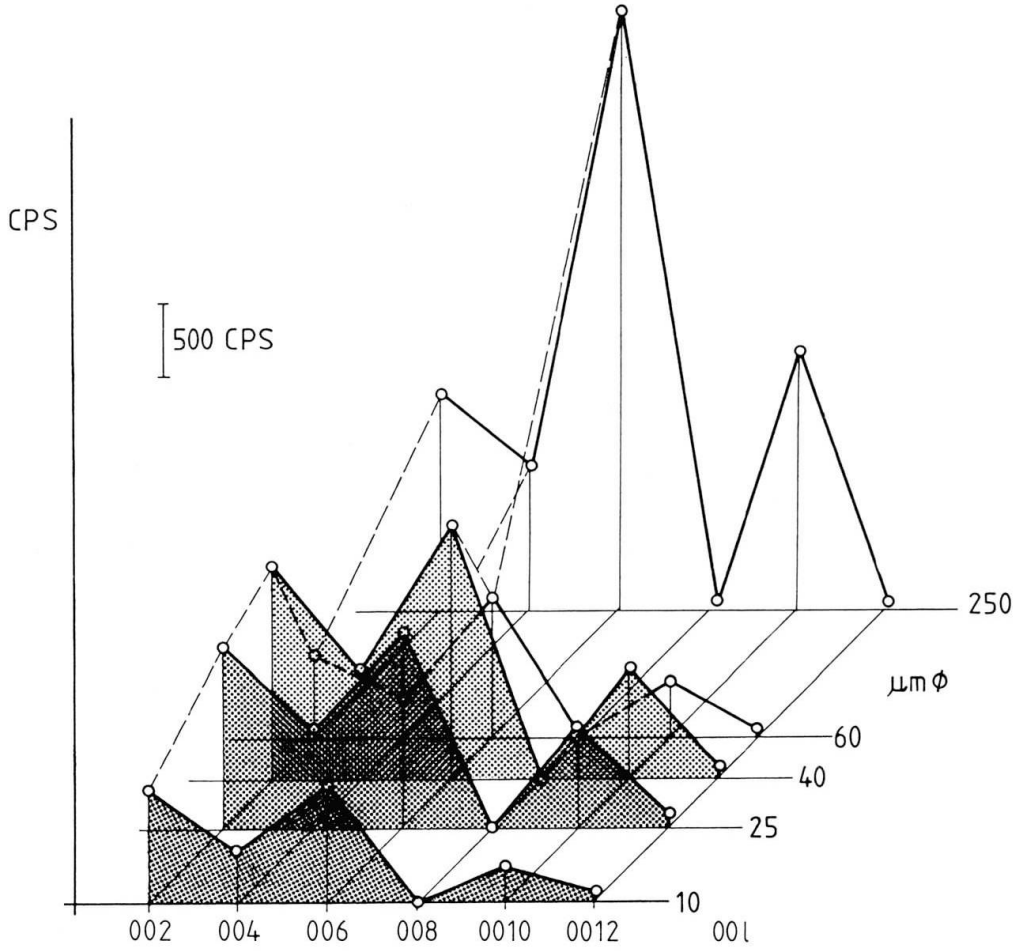

Fig. 6 a Absolute intensities of basal plane reflections (mica A-1) as a function of grain size (sieve fractions, µm ∅).

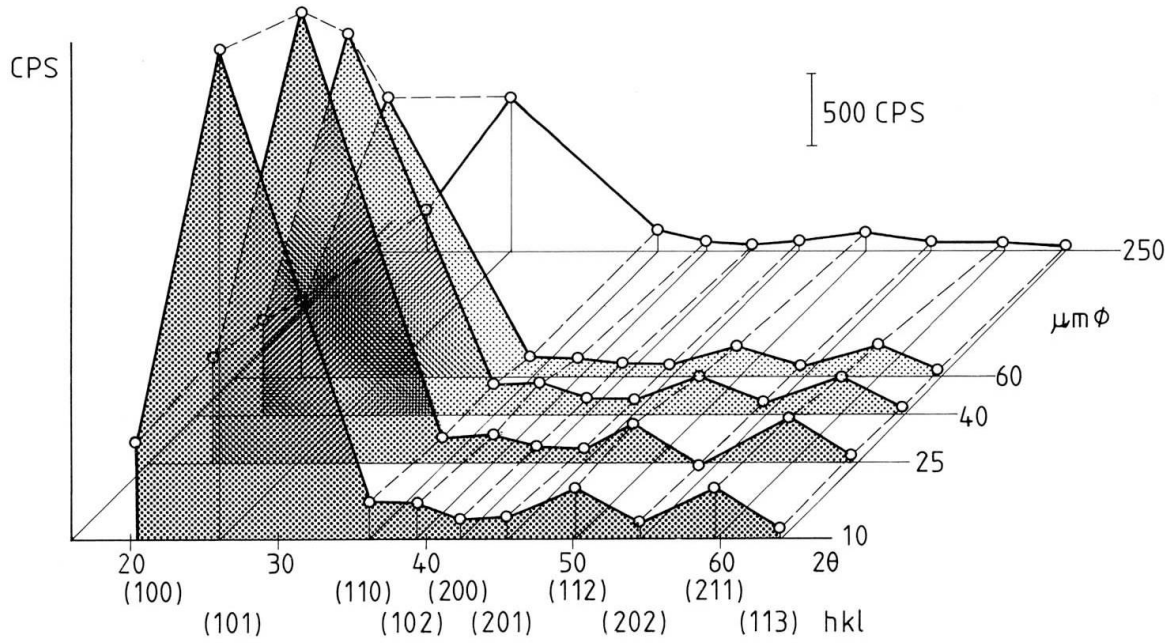

Fig. 6 b Intensity of diffraction peaks as a function of grain size: synthetic quartz.

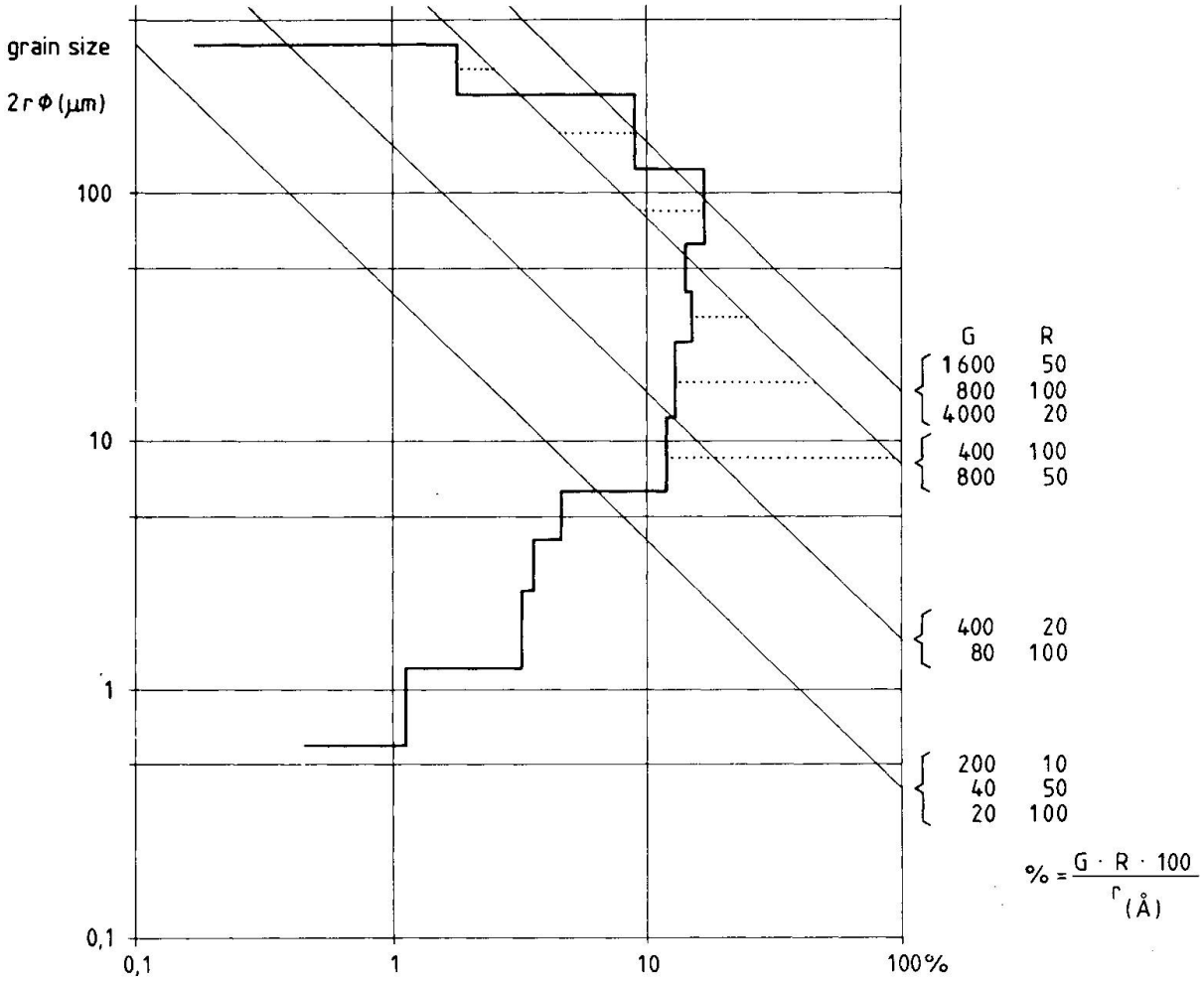

Fig. 7 Average grain size distribution, and calculated disordered percentage vs. grain size. For further explanation cf. (p. 155, 167).

A combination of grain size distribution and fractional lattice disordering by grinding is displayed on graph 7: the grain size distribution curve represents an average of muscovites of three different proveniences (A-1, C, E-3, sample A-1 ground respectively 2 and 17 minutes with a tungsten carbide disc mill, or 30 minutes with a steel disc mill).

The straight lines correlate the proportion of disordered lattice and the grain size of respective fractions based upon assumptions indicated on the right side of the graph. These assumptions are in detail

- cylindrical particles
- varying pile of disordered lattice cells on either side of a muscovite crystal (term "G"), Å
- varying radius to thickness ratio (term "R")

proportion of disordered to unaffected lattice volume-% $= \frac{G \cdot R \cdot 100}{r\,(Å)}$

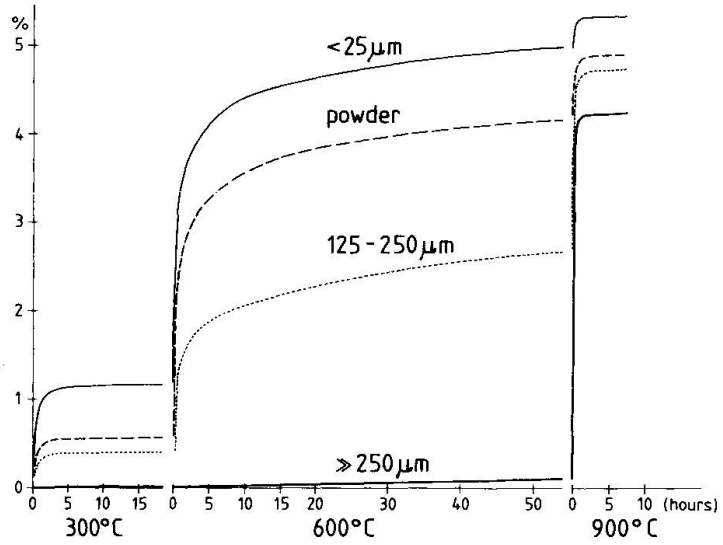

Fig. 8 Static TG: creeping weight loss at different temperatures. Powdered and single crystal sample of specimen A-1.

According to DTG/DTA runs muscovite fractions of grain sizes smaller than 25 µm∅ consist of nearly entirely disordered crystals since there are no more distinct peaks (dynamic run). A creeping weight loss at low temperatures (static TG, 300 °C, 600 °C, 900 °C, Fig. 8) is observed.

This creeping weight loss leads to an eventual complete dehydration of muscovite at low temperatures in function of grain size distribution and heating time.

These findings implicate:

- grain size has a crucial effect on thermal analyses; especially the appearance, shape and size of DTA/DTG peaks is not only a function of sample mass and chemical characteristics like volatile content but of granulometry as well;
- the calculation of thermodynamic properties based upon TG/DTA experiments might be affected by grain size, equilibrium conditions being, on their turn, dependent on time factors and granulometry.

As early as 1948/49 Roy has emphasized on the time factor being essential when conclusion from weight loss curves are drawn - an observation disregarded in many later publications.

A second, quite different, volatile free mineral - synthetic, hydrothermal quartz - has been examined in the same way, table 7.

Tab. 7 Cumulative grain size distribution of synthetic hydrothermal quartz. The amount of the cumulative percentage for the 25 µm fraction of 87% is due to losses of the finest particles during draining.

Milling time	>250	>125	>63	>40	>25	<25µm
2'	0	1	5	8	31	87
4'	0	0	3	7	29	87

The weight loss between 110°C and 1100°C was expectedly independent of the grain size and amounts to a value in the error range of the thermobalance ($\leq 0.2\%$).

The heat of reaction, high-low inversion at approx. 580°C of different size fractions and the reaction temperature (apex) is listed in Tab. 8.

The same tendency as for muscovite is observed: with increasing grain size the heat of reaction increases.

Tab. 8 Calculated heat of reaction, quartz

Reference	Ø (µm)	ΔH (J/g)	Z (°C)
Quartz	< 25	12.7	573 - 577
	> 25	13.8	577
	> 40	13.0	577
	> 63	15.2	577
	> 125	21.4	578
	> 250	20.2	578
	> 500	19.3	578

SMYKATZ-KLOSS, W. (1974) rsp. FAUST (1948) indicates 180 cal/mole = 12.6 J/g. The value is close to the < 25 µm fraction, a value being most probably too low. The statement of BAYLISS (1964, 1965) that the surface of the DTA-peak remains constant for particles ≥ 1 µm has not been confirmed.

Optical methods

The optical properties were determined by means of an immersion universal stage for grains mounted on a microscope with monochromatic-illumination (Na-light). For details: STECK et al. (1968).

Tab. 9 Optical properties of the examined muscovite samples. Accuracy of the refraction values: ± 0.002 (error of the immersion liquid: ± 0.001, error due to misorientation: ± 0.001).

Reference	2V	n_α	n_β	n_γ	Δ
A-1	39.9	1.555	1.585	1.593	0.038
B	41.0	1.552	1.581	1.590	0.038
D	42.0	1.562	1.589	1.598	0.036
E-3	42.0	1.556	1.585	1.596	0.040

Sample reference A-1 was submitted to a heat treatment. The main optical data and eventual observations are listed in Tab. 10.

Tab. 10 Optical properties of tempered muscovite reference A-1.

Heat treatment	2V	n_α	n_β	n_γ	observations
25°C	39.9	1.555	1.585	1.593	----
20' 650°C	40.0	1.553	1.586	1.593	----
20' 700°C	40.0	1.555	1.586	1.592	----
20' 750°C	39.0	1.554	1.583	1.593	striation
20' 800°C	36.4	1.553	1.583	1.593	striation, cloudiness
20' 850°C	37.0	?	?	?	striation, cloudiness
20' 900°C	34.8	?	?	?	striation, cloudiness

After a 20 minute heat-treatment at 750 °C the crystal shows a striation parallel to (010). With increasing temperature this structure gets more pronounced, furthermore rings of Newton are observed, probably due to the local release of water. The latter phenomenon develops into a disorderly cloudiness. The crystals lose their transparency and show a structure comparable to puff-pastry, the determination of the optical properties becomes impossible.

STÜTZEL (1954) describes a tendency of muscovite to become uniaxial in the temperature range of 600–1000 °C. When cooling the sample, it becomes biaxial again whereby the value of the optical axial angle decreases in function of its Fe-content. These observations have not been confirmed by the examined muscovites.

X-Ray Diffraction

Since the c-direction of a mica lattice might be affected by losses of cations in the interlayer and of hydroxyl loss as well (VEDDER, 1969), this basal spacing was examined by means of single crystal X-ray diffractometry. Sets of 001 reflexions of tempered (size 5 x 5 x 0.1 mm) and untempered mica crystals were examined and the c-parameter determined either by using high order reflexions (0020, 0022, 0024) and a graphical evaluation procedure (table 11, left row), or by calculating from the angular differences between neighbouring reflexions (STERN, 1977, NAEF, 1980), cf. table 11, right row.

In the temperature range between 700 and 900 °C the "normal", small, low-temperature spacing of 19.94 Å gradually disappears while a high temperature c with 20.11 Å is developping, cf. Fig. 9a, 9b. In the mentioned temperature

Tab. 11 c-Parameters of tempered micas (Å) (n.d. = not determined)

Mica	A-1		C-2		E-2	
25°C	n.d.	19.967	19.94	19.94	19.94	19.94
400°C	n.d.		19.94	19.944	19.94	19.945
600°C	n.d.	19.969	19.94	19.948	19.94	19.946
700°C	n.d.	19.974	19.94	19.947	19.94	19.946
800°C	n.d.	19.951	19.93	19.947	19.93	19.938
900°C	n.d.	20.112	20.11	20.110	20.15	20.111

range, two distinct lattices seem to exist. The disappearing low temperature spacing is correlated with a loss of volatile components occuring in the same interval (p. 150). Macroscopically, the flakes lose their transparency and become puff-pastry in shape. VEDDER (1969) states, extrapolating from VELDE (1966), that muscovite decomposes under atmospheric pressure (H_2O) at a temperature of about 600 °C, and that sanidine and corundum are formed.

Diffractometric studies on tempered samples (600–900 °C, single crystal and powder exposures) do not confirm crystallization of sanidine and/or corundum. Under atmospheric conditions only volatiles are released in the men-

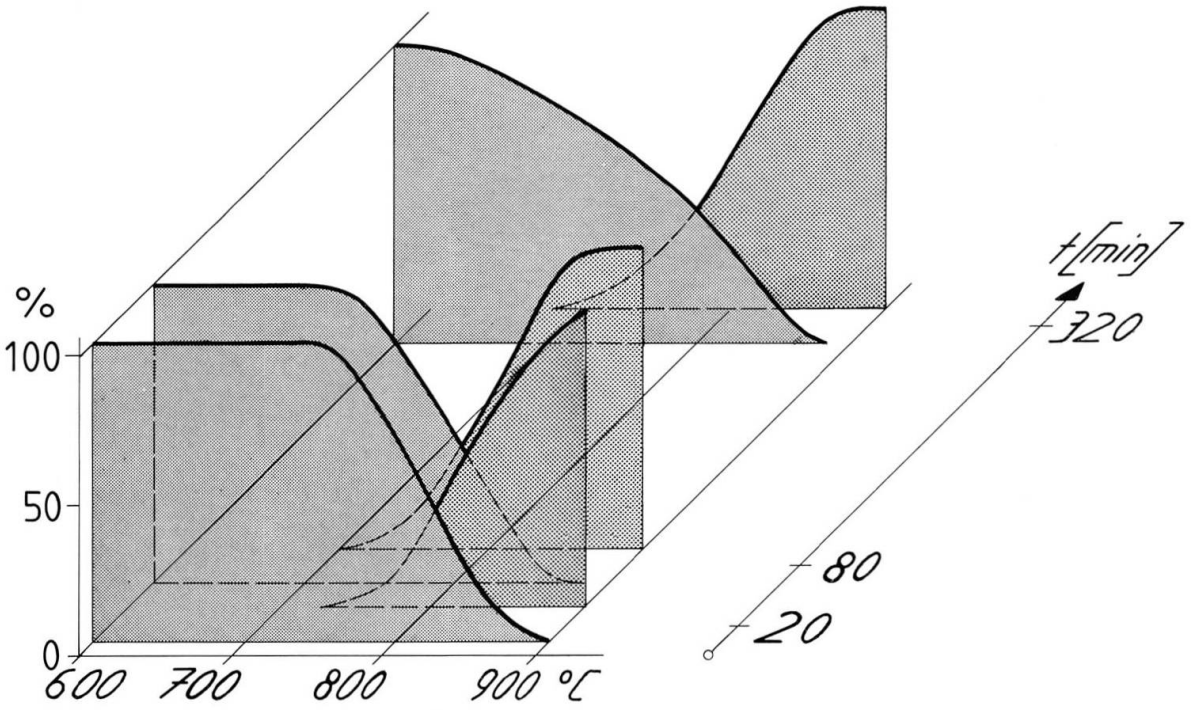

Fig. 9 a Intensity of mica 006 reflexions as a function of tempering temperature and time (mica A-1, single crystal diffractometry).

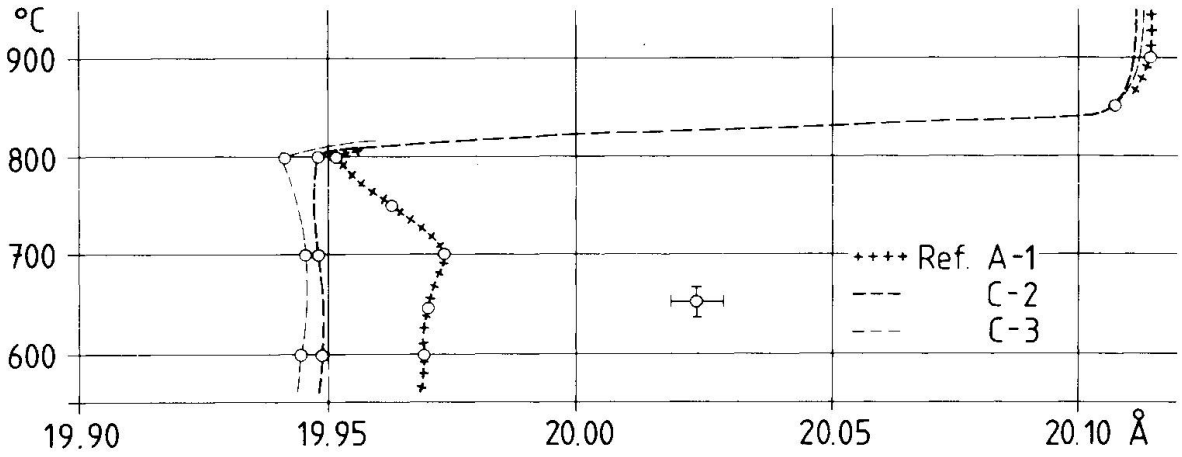

Fig. 9 b Low and high temperature lattices of tempered micas, c-parameter.

tioned temperature range, whereas the muscovite lattice decomposes above 1100 °C (endothermic DTA reaction at 1150 °C, cf. p. 148).

Powdered A-1 samples tempered at 1600 °C show a corundum phase in the melt.

Peak intensities (basal planes) of mica crystals from different proveniences may vary: neither the strongest reflexion (relative intensity = 100) is correlated with a specific order of reflextion, nor have specific reflexions similar intensities, e.g. the relative intensity of a (00 14) reflexion may vary from 1 to 8 according to sample provenience, table 12.

Intensities of basal reflexions, however, do not only behave differently in case of single crystals. Conventional powder diffractograms of samples having

Table 12 Relative peak intensities of tempered and untempered mica crystals from different proveniences.

reflexions	untreated micas				ignited 1 h at 900°C			
	A-1	B	D	E-2	A-1	B	D	E-2
002	42	40	35	35	42	75		
004	35	30	30	30	25	35		
006	85	100	100	100	100	100	100	100
008	19	16	14	18	14	12	15	13
0010	100	71	80	90	19	16	17	19
0012	2	2	1	1	2	1	2	2
0014	1	8	5	4	2	2	2	2
0016	15	13	7	11	2	1	2	2
006/0010	.85	1.43	1.25	1.11	5.26	6.25	5.88	5.26

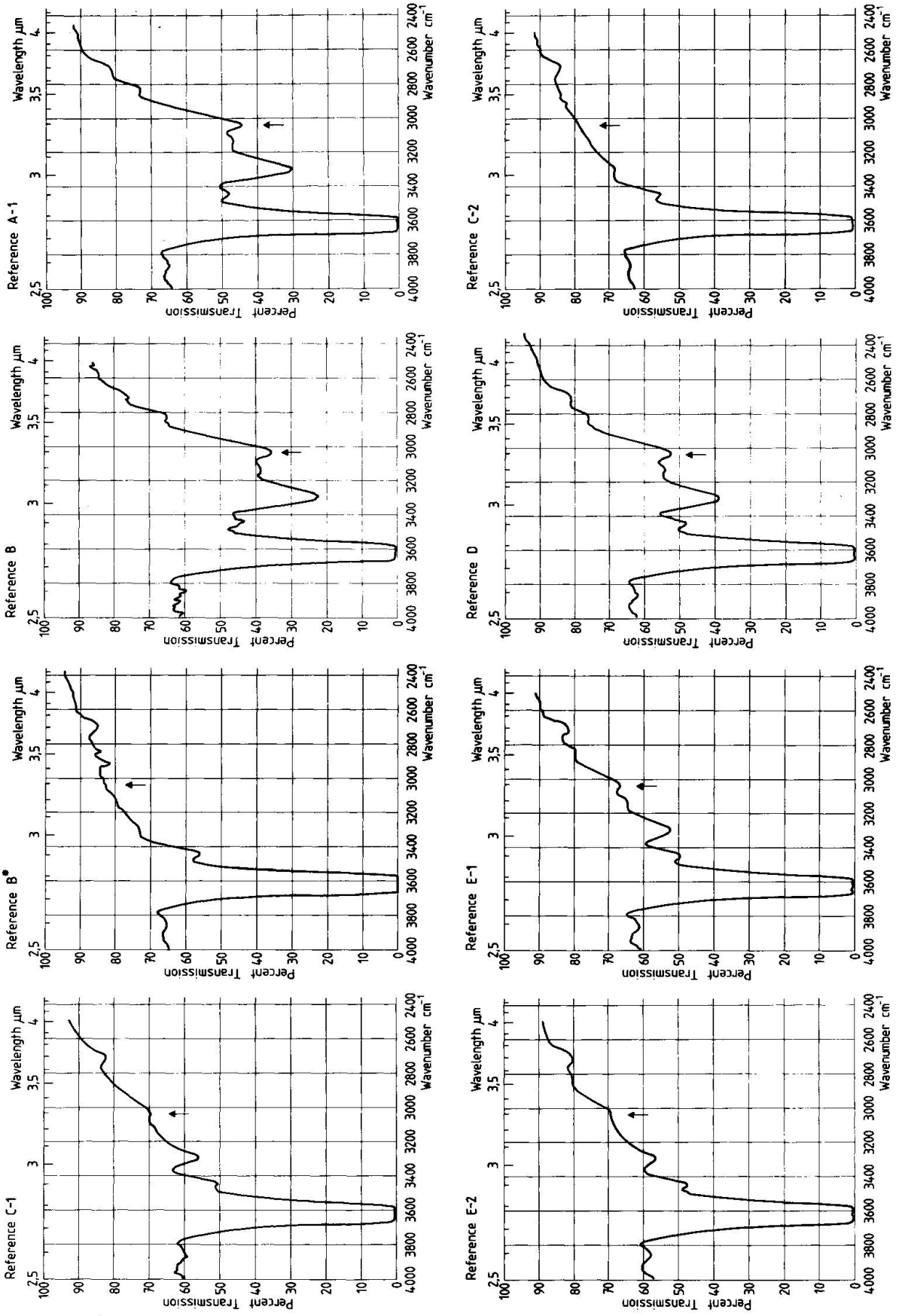

Fig. 10 IR absorption spectra of the examined muscovites.

different grain sizes (sieve fractions) generally show decreasing absolute intensities of small fractions in case of mica specimen A-1 (Fig. 6a) but of increasing values in case of a synthetic quartz (Fig. 6b).

Infra-red spectroscopy

The infra-red absorption spectra between 4000 and 2500 cm^{-1} (2.5–4 μm) of the examined muscovites show different patterns (Fig. 10 and Tab. 13).

Table 13 Absorption bands of the examined muscovites at room temperature, B*: typical spectrum of Madras green mica; vs: very strong, s: strong, m: medium, w: weak, d: detectable.

	A-1	B	B*	C-1	C-2	D	E-1	E-2
3630 cm^{-1}	vs	vs	vs	vs	vs	vs	vs	vs
3420	w	w	w	d	d	w	w	d
3300	s	s	-	m	d	s	m	m
3100	d	-	-	-	-	d	-	-
3040	w	w	-	d	-	w	d	d
2830	d	d	-	-	-	d	-	-
2700	-	-	w	w	w	d	w	w

All the observed frequencies, with the exception of the 3040 cm^{-1} band, are assigned to OH-stretching vibration according to SERRATOSA et al. (1958) and VEDDER (1964).

The absorption at 3040 cm^{-1}, once characteristic for ruby muscovite originating from Bihar, vanishes when heated up to approx. 220 °C, whereas a second absorption appears at 2680 cm^{-1}. The original room temperature pattern is instantly obtained by cooling.

The disappearance of the 3040 cm^{-1} band and the appearance of the band at 2680 cm^{-1} is reversible and therefore a physical phenomenon. The change of the extinction in function of the temperature is linear. Similar observations of a linear decrease of the OH-absorption with increasing temperature were made by FINCH et al. (1956), HUGHES et al. (1956) and LIDDEL et al. (1957) with simple C-O -H systems.

VEDDER, (1965), associates the absorption bands of a Bengal ruby muscovite sample in the lower frequency part of the 2800–3400 cm^{-1} system with ammonium. Although the studied Bihar sample shows a comparable IR-spectrum, ammonium was not detected. According to Vedder the 2710 rsp. 2680 cm^{-1} band is due to a combination of stretching and liberation motion of the OH-ions. Fig. 2 in VEDDER, (1956), also displays an intensity variation with changing tempera-

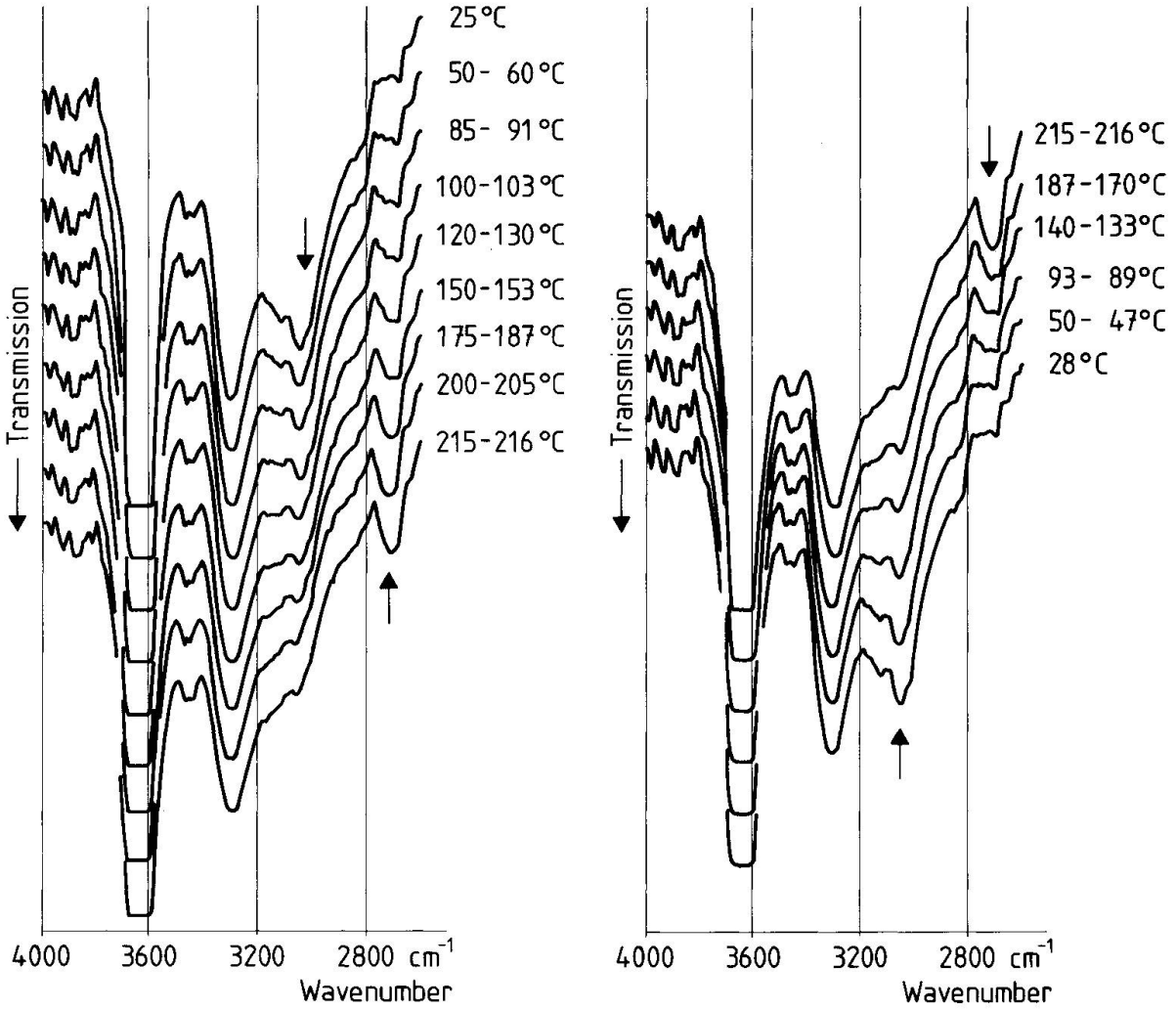

Fig. 11 Temperature dependence of the IR spectrum of mica sample A-1 on heating and cooling.

ture for the 3040 cm^{-1} band attributed to ammonium. Due to the direct relation between the disappearance of the 3040 cm^{-1} band and the appearance of the 2680 cm^{-1} band this observation is associated to a combined OH-motion.

The existence of ammonium in muscovite might be possible but can neither be attributed to the 3040 cm^{-1} band nor to a low occupancy of interlayer sites. The determined NH_4-content of VEDDER (1965) is too low to compensate these sites. Contrary to any literary reference the 3040 cm^{-1} frequency band may also occur in IR-spectra of muscovite originating from other proveniences.

X-ray fluorescence investigation

A set of 22 mica samples has been analyzed by means of conventional wavelength dispersive X-ray fluorescence (WDS-XRF), table 14. The highest num-

ber (11) comes from Sudan since not much is known on the chemical composition of Sudanese micas - the United Nations technical report (1972) on mica from northern Sudan does not refer to a single analysis, whereas data on micas from India exist (p. 146).

Since optical and X-ray diffraction data of mica from different proveniences do not vary widely, the chemical composition of the studied samples was expected to be quite homogeneous, too.

The structural formulae of ideal white mica (i.e. muscovite s.s.) contains 6 Si and 2 Al atoms per unit cell in tetrahedral (Z) site, 4 Al atoms in octahedral (Y) site and 2 K atoms in the interlayer (X) site.

The octahedral Al of real white micas, however, is partially replaced by Mg, Fe, Mn, etc., correspondingly the tetrahedral Si/Al ratio changes due to valence compensation. The nomenclature of these white micas is not well established since pure end members of solid solution series do practically not occur; the following names are common:

site	ideal muscovite	phengitic muscovite	paragonitic muscovite	margaritic muscovite
X	2K	2K, or K ⇌ Na	K ⇌ Na	K ⇌ Ca
Y	4Al	Al ⇌ Mg, Fe	4Al	4Al
Z	6Si 2Al	Si ⇌ Al, Ti	6Si 2Al	6Si 2Al
	14	14	14	14 sum of cations per unit cell

Most common are phengitic muscovites, accordingly, a triangular plot of octahedral occupancies demonstrates best the variation of natural white mica, Fig. 12. The examined Bihar muscovites contain the lowest amount of phengitic components, certain Rajasthan- and Sudanese micas the highest concentration.

In cases where steel mills are used for grinding mica crystals, an artifical "phengitization" may take place: the iron content of muscovite increases parallel to grinding time. In consequence, attention should be paid to grinding techniques when quoting published analytical data. Using tungsten carbide or agate milling devices is the most suitable way to avoid iron contamination.

Several mica crystals have been examined by direct surface analysis using an energy dispersive X-ray fluorescence technique (EDS-XRF), for analytical details cf appendix. Advantages of EDS-XRF: analytical information comes in simultaneously and data evaluation is fast thanks to appropriate computer facilities handling the energy spectra and printing out count rates for chemical elements present in a sample.

Count rates, however, may only be directly compared to each other if either chemically and physically similar samples are analyzed, or if effects of chemical and physical differences are compensated by mathematical absorption corrections and/or by preparative tricks like sample dilution, etc.

As to micas, a special point of interest is the eventual replacement of potassium by rubidium according to environmental conditions of mica genesis: Rb-rich melts of magmatic origin might favour the growth of prospectively Rb-rich minerals like micas or orthoclase, whereas minerals of metamorphic-anatectic origin are possibly poorer in Rb, thus resulting in high K/Rb ratios.

Direct surface analysis of mica presents some technical difficulties as to the critical depth: the absorption of high energy radiation is weaker than the one of low energy. The depth interval may vary from several Ångströms (energies $<<$ 1 KeV, i.e. K_α radiation of elements with $Z < 9$) to several hundreds of microns (energies $\geqq$ 5 to 10 KeV, K_α radiations of elements with $Z \sim 30$). The critical thickness, however, is not only a function of energy but of absorption capability of the sample as well. Fortunately, mica is a very suitable material for checking the critical depth: a mica book with an initial thickness of several millimeters was split up step by step; after each splitting its thickness was measured and an energy spectrum recorded of the same sample area. Thus, count rates of specific elements eventually began to drop when the respective critical thickness was reached. In case of white mica, thickness becomes critical for iron (K_α = 6 KeV) at approx. 100 μm whereas for magnesium (K_α = 1,3 KeV) critical thickness is below 20 μm. Extrapolating these figures towards higher energies, one may assume that for most analytical conditions a sample thickness above 300 μm (0.3 mm) is sufficient.

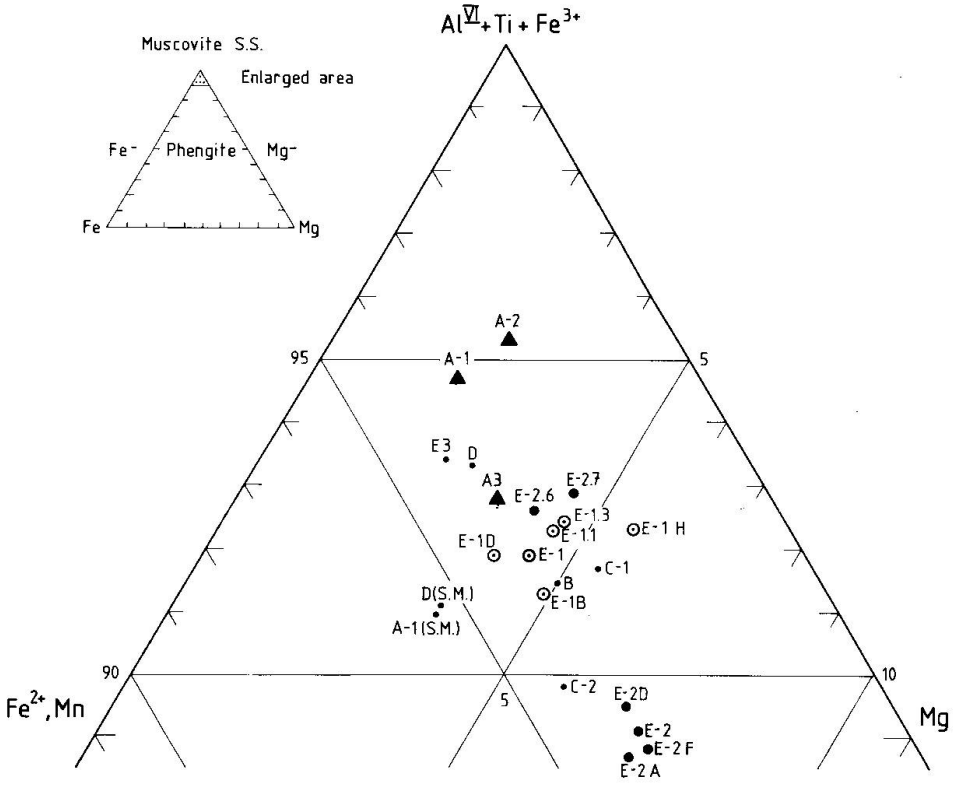

Fig. 12 Triangular plot of muscovite, octahedral occupancies (S. M. = steel mill).

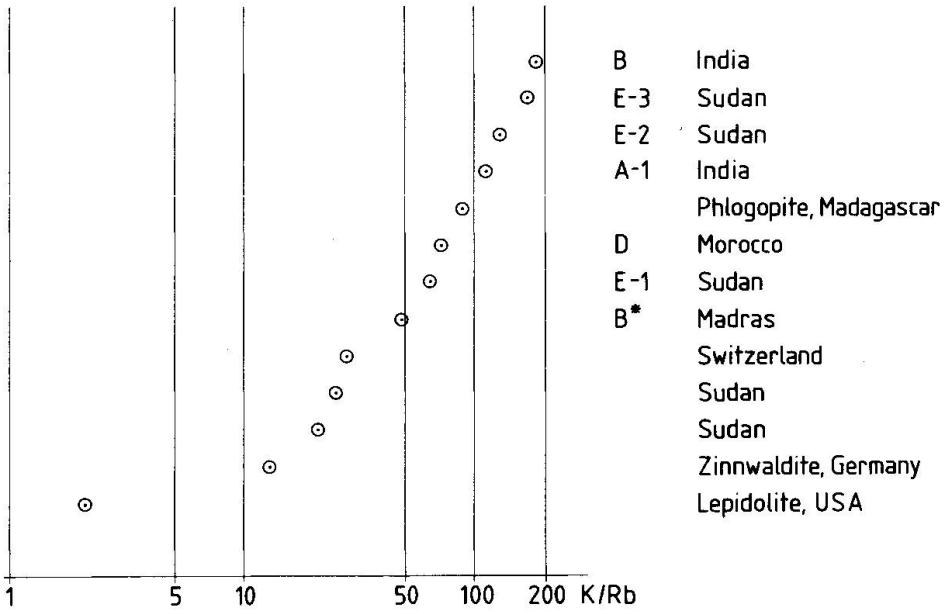

Fig. 13 K/Rb ratios of white micas from different origin (EDS-XRF)

This implies that a direct surface analysis of minerals (element ratios and not absolute concentrations) seems possible when
- the sample thickness is greater than 0.3 mm
- the sample surface is flat

Potassium/rubidium ratios of micas from different proveniences are presented in Fig. 13. The K/Rb ratios roughly vary from 20 to 200; where the border line between micas of magmatic vs metamorphic genesis might be drawn is at present uncertain. It shall be subject of future studies.

The limited number of samples per mining site does not allow an estimation of chemical variation within a specific occurrence. Only in the case of Sudanese micas from the Shereik area an observation on chemical variation seems justifiable: samples taken in winter 1979 contain slightly more iron and magnesium than those collected in winter 1980 (after one year of further exploitation). Whether this observation is firmly established or not remains open. In literature, consequent studies on chemical variability of ruby micas from one and the same pegmatitic site are lacking.

Discussion and conclusion

Literature on physical properties of mica is fairly numerous; most of the data, however, were published before 1965. A recent computer-based review revealed no significant literature for the past five years on these matters.

Several questions are still open:

- what does determine peak size and shape of TG and DTA reaction?
- which kind of relation exists between IR spectrometrical and chemical data, origin of muscovite, rsp.?
- are there connections between X-ray diffraction pattern of muscovite and TG or grain size distribution?

Static experiments show a gradual, creeping weight loss over a wide temperature range in regard to fine grain size fractions. The latter generally release a higher amount of volatiles than coarser fractions.

The difference in weight loss of max. 20–25% relative remains up to the melting point of the muscovite sample at 1600°C and is due to a partial release of the alkalies: XRF analysis of a tempered muscovite (A-1, grain size < 25 µm ∅ tempered at 1320°C) shows a loss of 1.3 weight % K_2O.

Dynamic experiments (DTA/TG) display two distinct endothermic DTA-peaks, the one at approx. 850°C combined with a clear weight loss (DTG peak), therefore, assigned to the dehydration of muscovite; the other at 1150°C without any weight loss. For that reason the latter reaction is associated with the decomposition of muscovite. The endothermic reaction at around 850°C vanishes in small grain fractions, the apex shifts in function of grain size, too – in contrast to findings of HOLT et al. (1957). The exothermic reaction at around 300°C (BISHUI et al., 1961) has not been confirmed by the specimens examined so far.

The creeping weight loss and the disappearance of the endothermic peak at 850°C with decreasing grain size is best explained by the high percentage of disordered or destroyed lattice proportions: assuming e.g. a radius/thickness ratio of 100, and a pile of 20 disturbed unit cells on either side of a muscovite flake, approx. 50% of a 40 µm fraction is affected, and therefore dehydrated at relatively low temperatures.

Thermodynamic results (temperature of reaction, TG, DTA and thereof deduced values like heat of reaction, etc.) without the experimental details as recommended by LOMBARDI (1977) as well as details of grain size distribution represent arbitrary data.

Apparently based on YODER et al. (1966) and VELDE (1966) certain authors assume the decomposition temperature of muscovite being at 600°C . There even exists a confusion of terms: the decomposition and the dehydration of mica in function of the temperature under atmospheric pressure is not identical; e.g. SMYKATZ (1974) indicates the decomposition temperature of muscovite at 887°C. The influence of time is often neglected.

Based on microscopical (STÜTZEL, 1954; SABATIER, 1955) and IR-spectroscopical (GAINES, 1964) observations Sabatier and Gaines propose a multi-step dehydration reaction including the formation of water molecules from structural OH-groups as a local and reversible reaction at temperatures ≤ 650°C and

Tab. 14 Chemical analyses and structural formulae of the examined muscovites (cf. 146). E-1 rsp. E-2 represents the mean value of three individual samples originating from trench B, D and H rsp. A, D and F (depth: 2 m) perpenticular to the pegmatitic body. E-1.1, E-1.3, E-2.6 and E-2.7 were sampled in lower levels (2–10 m).

	A-1	A-2	A-3	B	C-1	C-2	D	E-1	E-1.1	E-1.3	E-2
Weight-%											
SiO_2	47.3	46.0	45.5	46.0	45.4	45.8	47.2	45.5	45.2	44.3	45.6
Al_2O_3	33.8	35.2	33.7	33.5	35.5	34.2	34.7	34.7	34.2	34.5	33.4
Fe_2O_3	.6	1.27	2.05	.7	.9	.9	.7	1.23	1.1	1.65	1.10
FeO	1.20	.8	1.3	1.30	1.00	1.50	1.40	1.27	1.1	1.0	1.23
MnO	.01	.03	.04	.0	.07	.08	.00	.10	.03	.03	.09
MgO	.4	.5	.7	1.0	1.1	1.2	.6	.9	.9	.9	1.47
CaO	.00	.04	.05	.00	.14	.14	.00	.14	.14	.20	.16
Na_2O	.60	.8	.8	.7	.8	.4	.6	.4	.7	.9	.47
K_2O	10.23	9.74	10.11	10.03	10.15	10.59	10.36	10.51	10.60	10.70	10.61
TiO_2	.53	.44	.38	.50	.23	.32	.25	.22	.17	.10	.45
H_2O	4.80	4.9	5.0	5.20	4.70	4.80	4.90	4.90	5.6	5.1	4.80
	99.47	99.72	99.63	98.93	99.99	99.93	100.71	99.86	99.74	99.38	99.41
Structural formulae (based upon 14 cations)											
Si	6.38	6.179	6.142	6.246	6.038	6.132	6.278	6.103	6.10	5.96	6.134
Al	5.37	5.571	5.361	5.36	5.563	5.396	5.439	5.493	5.44	5.47	5.300
Fe^{3+}	.060	.128	.208	.071	.09	.09	.07	.124	.111	.166	.111
Fe^{2+}	.135	.089	.146	.147	.111	.167	.155	.142	.124	.112	.138
Mn^{2+}	.001	.003	.004	.000	.007	.009	.000	.011	.003	.003	.010
Mg^{2+}	.08	.100	.140	.202	.217	.239	.118	.179	.18	.18	.293
Ca^{2+}	.0	.005	.007	.0	.019	.020	.0	.019	.020	.028	.023
Na^{+}	.156	.208	.209	.184	.206	.103	.154	.104	.18	.23	.121
K^{+}	1.759	1.668	1.740	1.736	1.721	1.808	1.757	1.799	1.823	1.835	1.820
Ti^{2+}	.053	.044	.038	.051	.022	.032	.024	.022	.017	.010	.045
OH	4.318	4.39	4.502	4.709	4.169	4.286	4.347	4.387	5.04	4.58	4.307
Al^{IV}	1.619	1.820	1.857	1.753	1.961	1.867	1.721	1.896	1.90	2.04	1.865
Al^{VI}	3.752	3.751	3.504	3.606	3.602	3.528	3.718	3.597	3.54	3.43	3.435
oct	4.083	4.117	4.042	4.079	4.052	4.067	4.087	4.076	3.97	3.90	4.035
alc	1.916	1.882	1.957	1.920	1.947	1.932	1.912	1.923	2.03	2.10	1.964
% Fe^{3+},Al,Ti	94.7	95.3	92.8	91.4	91.7	89.8	93.3	91.9	92.3	92.4	89.1
% Fe^{2+},Mn	3.3	2.2	3.7	3.6	2.9	4.3	3.8	3.8	3.2	2.95	3.7
% Mg	2.0	2.4	3.5	5.0	5.4	5.9	2.9	4.4	4.5	4.6	7.3
d	2.791	2.812	2.857	2.761	2.807	2.818	2.780	2.805	-	-	2.809

the final dehydration reaction inducing the delamination of the mica by the water pressure inside the crystal. This interpretation could not be confirmed.

IR spectroscopic data have been reported to indicate a specific provenience of muscovite since typical Bihar ruby muscovite shows a distinct IR peak at 3040 cm^{-1} (SERRATOSA et al., 1958) allegedly due to replacement of potassium by ammonium in their interlayer (VEDDER, 1965). Most probably, micas do contain NH_4^+ sometimes, either replacing alkalies or hydroxyl ions, but published quantitative data seem to be lacking so far. The implicitely quoted ammonium content of max. 0.2% (VEDDER, 1965) for certain Bihar muscovites is not sufficient to compensate for their low alkali occupancy of the structural formula

E-2.5	E-2.7	E-3	E-1B	E-1D	E-1H	E-2A	E-2D	E-2F	A-1(S.M.) Steelmill	D(S.M.) Steelmill
45.0	44.0	46.6	45.5	45.5	45.4	46.2	45.6	45.0	46.4	45.2
35.0	35.1	34.0	34.5	34.8	34.90	33.2	33.5	33.6	33.7	33.5
.5	2.1	.7	1.10	1.20	1.40	1.10	1.10	1.10	.80	.20
1.1	.9	1.50	1.30	1.40	1.10	1.30	1.20	1.20	1.40	1.90
.04	.03	.00	.09	.10	.10	.09	.09	.09	.01	.01
.8	.9	.5	1.0	.8	.9	1.5	1.4	1.5	.2	.7
.25	.17	.00	.13	.14	.14	.15	.16	.17	.00	.00
.8	.8	.7	.5	.3	.4	.5	.4	.5	.5	.7
10.92	10.25	10.30	10.49	10.55	10.50	10.62	10.70	10.51	10.12	10.16
.03	.38	.10	.22	.20	.23	.40	.48	.48	.52	.26
5.3	5.5	5.30	4.70	4.90	5.10	4.80	4.70	4.90	5.50	6.00
99.74	100.13	99.70	99.53	99.89	100.17	99.86	99.33	99.05	99.15	98.63
6.03	5.91	6.287	6.108	6.113	6.087	6.188	6.137	6.078	6.340	6.205
5.52	5.56	5.405	5.457	5.509	5.514	5.240	5.312	5.347	5.426	5.419
.050	.212	.071	.111	.121	.141	.110	.111	.111	.082	.020
.123	.101	.169	.145	.157	.123	.145	.135	.135	.159	.218
.004	.003	.000	.010	.011	.011	.010	.010	.010	.001	.001
.16	.18	.100	.199	.160	.179	.299	.280	.301	.040	.143
.035	.024	.00	.018	.020	.020	.021	.023	.024	.000	.000
.21	.21	.183	.130	.078	.103	.129	.104	.130	.132	.186
1.865	1.757	1.772	1.795	1.807	1.795	1.813	1.836	1.810	1.763	1.778
.003	.038	.01	.022	.020	.023	.040	.048	.048	.053	.026
4.73	4.93	4.769	4.208	4.391	4.561	4.288	4.219	4.414	5.012	5.494
1.97	2.09	1.712	1.891	1.886	1.912	1.811	1.862	1.921	1.659	1.794
3.55	3.47	3.693	3.566	3.623	3.601	3.428	3.450	3.426	3.766	3.625
3.89	4.01	4.044	4.055	4.094	4.080	4.034	4.036	4.034	4.104	4.035
2.11	1.99	1.955	1.944	1.905	1.919	1.965	1.963	1.965	1.895	1.964
92.6	92.9	93.3	91.3	92.0	92.3	88.7	89.5	88.9	95.1	91.0
3.3	2.6	4.2	3.8	4.1	3.3	3.8	3.6	3.6	3.9	5.4
4.1	4.5	2.5	4.9	3.9	4.4	7.4	6.9	7.5	1.0	3.5
-	-		2.800	2.806	2.810	2.809	2.803		-	-

(1.9 K, Na instead of 2.0) and can, therefore, not be fully explained by K/NH_4^+ replacement.

Furthermore, tempering studies executed on Bihar ruby mica show a linear correlation of the decreasing 3040 cm^{-1} ("ammonium") band and of an increasing 2680 cm^{-1} band in a temperature range of 28 to 216 °C. These reactions are reversible and, therefore, not based on a chemical but on a physical effect.

Finally, the "Bihar" peak at 3040 cm^{-1} was observed on ruby muscovites from several other proveniences, obviously a quite common phenomenon not restricted to Bihar micas.

Powder X-ray diffractometry of different grain size fractions expectedly

shows no peak shift phenomenon. Peak intensities of fine fractions (< 25 μm) generally are much weaker than those of coarser ones (> 125 μm). This observation is in contrast to results obtained on synthetic quartz.

X-ray diffractometry executed on tempered single crystals (basal reflexions) displays a normal c-parameter up to a temperature of slightly over 800 °C. Parallel to the vanishing normal cell parameter of ~ 19.94 Å a high temperature cell with c ~ 20.1 Å develops. Simultaneously the mica crystal loses its transparency and becomes puff-pastry in shape. This phenomenon is obviously correlated with the water release of coarse grained crystals.

Under atmospheric conditions, a decomposition of muscovite and a formation of corundum + sanidine obviously does not take place at about 850 °C but the formation of a somewhat larger muscovite lattice which probably disappears only above 1150 °C. At a tempering temperature of ~ 1300 °C the diffractogram of A-1 muscovite (< 25 mm ∅) does not clearly show identifiable peaks; especially, no corundum reflexions have been found. Sample A-1 tempered at the melting temperature of ~ 1600 °C, however, contains corundum according to diffractometric investigations.

The chemical variability of muscovite is supposed to be relatively small. A partial replacement of octahedral Al by Mg, Fe leads to a phengitic composition being to a certain degree connected with the mica origin: Bihar muscovite is remarkably pure, i.e. nearly Mg-, Fe-free, whereas certain mica (e.g. from Sudan) show a higher phengite content.

Since chemical data on technically used mica are astonishingly scarce and their natural variability is virtually unknown, no ascertained statements on mica composition vs origin are possible, except for certain Sudanese micas where samples from one and the same site were taken and analyzed (specimen series «E»).

The comparison and evaluation of published analyses turn out to be difficult since structural formulae of mica, taken from literature, are calculated on a sum of either 22 oxygen, or mostly of 24 (O, OH . . .). Neither oxygen nor OH are - if analyzed at all - determined accurately. Especially the quite considerable error of water determination affects an anion-based structural formula considerably (STERN, 1979). Thus, a calculation based upon 14 cations seems preferable (table 14).

The potassium/rubidium ratio of mica crystals from different origin was investigated by direct EDS-XRF surface analysis. This ratio varies from approx. 20 to 200 and is eventually linked with mica genesis/provenience: pegmatites rich in rare minerals/elements may contain more rubidium than pegmatites of metamorphic-anatectic origin poor in rare minerals.

Acknowledgement

The authors are indebted to the Swiss Insulating Works for supporting this study.

Literature

BARDET, J.J. (1945): Methods for treating mica and composition. US Pat. 2549880.

BAYLISS, P. (1964): Effect of particle size of differential thermal analysis. Nature *4923.*

BAYLISS, P. (1965): Differential thermal analysis: Effect of particle size. Nature *207,* 284.

BISHUI, B.M., DAR, R.N. and MANDAL, S.S. (1961): Studies on Indian mica: effect of dry grinding on DTA. Central Glass and Ceram. Research Inst., Bull. *8,* No. 1, 15–22.

BOULADON, J, JOURAVSKI, G. et MORIN, P.(1950): Etude préliminaire des pegmatites à muscovite et béryl du sud de la plaine de Tazenatekt. Notes et mém. No 76. Serv. géol. du Maroc *3,* 207–235.

CHOUBERT, G. (1969): Histoire géologique de l'anti-Atlas de l'archéen à l'aurore des temps primaires. Série A, No 4383, Fac. Sci. Univ. Paris.

DATTA, A.K. (1973): Internal structure, petrology and mineralogy of calcalkaline pegmatites in parts of Rajasthan. Mem. Geol. Surv. India, *102.*

DUNN, J.A. (1961): Mica. Bull. Geol. Surv. India, Series A-19.

FAUST, G.T. (1948): Thermal analysis of quartz and its use in calibration in thermal analysis studies. Amer. Mineralogist 33, 337–345.

FINCH, J.N. and LIPPINCOTT, E.R. (1956): Hydrogen Bond Systems: Temperature dependence of OH frequency shifts and OH band intensities. J. Chem. Phys. *24,* 908–909.

GAINES, G.L. and VEDDER, W. (1964): Dehydroxylation of muscovite. Nature *4918,* 495.

HEYMANN, M.D. (1943): Integrated mica and method of making the same. US Pat. 2405576.

HOLT, J.B., CUTLER, I.B. and WADSWORTH, M.E. (1957): Rate of thermal dehydration of muscovite. J. Amer. Ceramic Soc., *41,* 7, 242–246.

HUGHES, R.H., MARTIN, R.J. and COGGESHALL, N.D. (1956): Temperature dependence of indrared absorption. J. Chem. Phys. *24,* 489–490.

HUTCHISON, C.S. (1974): Laboratory handbook of petrographie technique. John Wiley and Sons, New York.

KABESH, M.L. (1960): Mica deposits of northern Sudan. Geol. Surv. of Sudan, Bull. 7.

LIDDEL, U. and BECKER, E.D. (1957): Temperature-dependent absorption by CH_3OH and $CHCl_3$ in the 3 μ region. J. Chem. Phys. *25,* 173–174.

LOMBARDI, G. (1977): For better thermal analysis. Istituto Min. Petr. Univ. Roma.

MACKENZIE, R.C. and MILNE, A.A. (1953): The effect of grinding on micas. I. Muscovite. Min. Mag. *30,* 178–185.

MAHADEVAN, T.M. and MAITHANI, J.B.P. (1961): Geology and petrology of the mica-pegmatites in parts of the Bihar mica belt. Mem. Geol. Surv. India, *93.*

NAEF, U. (1980): Über eine Korrelation von physikalischen und chemischen Grössen bei Hellglimmern. Diplomarbeit Univ. Basel.

NAEF, U. and STERN, W.B. (1982): Some critical remarks on the analysis of phengite and paragonite components in muscovite by X-ray diffractometry. Contrib. Mineral. Petrol 79 (in press).

PARKERT, C.W., PERKINS, A.T. and DRAGSDORF, R.D. (1950): Decomposition of minerals by grinding. Trans. Kansas Acad. Sci. *53,* 3, 386–397.

ROY, R. (1949): Decomposition and resynthesis of the micas. J. Amer. Ceramic Soc. *32,* 6, 202–209.

SABATIER, M.G. (1955): Les transformations du mica muscovite aux environs de 700°C. Bull. Groupe Franc. Argiles, *6,* 35–39.

SCHULTZE, D. (1969): Differentialthermoanalyse. Berlin.

SERRATOSA, J.M. and BRADLEY, W.F. (1958): Infrared absorption of OH bonds in micas. Illinois State Geol. Surv., Urbana Nor. 4602, 111.

SKOW, M.L. (1962): Mica, a material survey. US Dept. of the Interior Bureau of Mines, Inf. Circ. 8125.

SMYKATZ-KLOSS, W. (1974): Differential thermal analysis. Springer, Berlin, Heidelberg, New York.

STECK, A. und GLAUSER, E. (1968): Universaldrehtisch für optische Untersuchungen von Mineralkörpern. Schweiz. mineral. petrogr. Mitt. *48*, 815–820.

STERN, W.B. (1977): A camera attachment for X-ray diffractometry of minute mineral samples. Schweiz. mineral. petrogr. Mitt. *57*, 291–298.

STERN, W.B. (1979): Zur Strukturformelberechnung von Glimmermineralien. Schweiz. mineral. petrogr. Mitt. *59*, 75–82.

STERN, W.B. (1979): Probleme der quantitativen röntgenspektrometrischen Analyse von Hauptkomponenten und Spuren in geologischen Proben. Schweiz. mineral. petrogr. Mitt. *59*, 83–93.

STÜTZEL, A. (1954): Untersuchungen am Muskovit. Diss. Eberhard-Karls-Univ., Tübingen.

UN-Report (1972): Mineral survey in three selected areas: Sudan, vol. 2, Prospecting for mica in the Shereik area, northern Sudan. DP/SF/UN/79 Tech. Rep. 2.

VEDDER, W. (1964): Correlations between infrared spectrum and chemical composition of mica. Amer. Mineralogist *49*, 736–768.

VEDDER, W. (1965): Ammonium im muscovite. Geochim. cosmochim. Acta, *29*, 221–228.

VEDDER, W. (1969): Dehydroxylation and rehydroxylation, oxidation and reduction of micas. Amer. Mineralogist *54*, 482–509.

VELDE, B. (1966): Upper stability of muscovite. Amer. Mineralogist, *51*, 924–929.

YODER, H.S. and EUGSTER, H.P. (1955): Synthetic and natural muscovites. Geochim. cosmochim. Acta, *8*, 225–280.

Appendix: Technical Data

Ia Thermal Analysis: Differential Thermal Analysis

Apparatus:	Thermobalance Mettler TA 2
Sample weight:	60–63 mg, no dilution, reference: calcined Al_2O_3
Sample holder:	Pt, form: cone, volume: 0.1 cm^3, Pt-Rh-Pt-thermocouple, sample atmosphere: air, 4 l/min
Furnace:	medium temperature, heating rate: 10 °C/min, isothermic at 110 °C until no weight loss is observed (moisture), maximum temperature: 1200 °C
DTA-range:	50 μV, TG-range: 10 mg/1mg, DTG-range: 1 mg/min

Ib Thermal Analysis: Thermogravimetry

Apparatus:	Thermobalance Mettler TA 2
Sample weight:	700–800 mg
Sample holder:	Al_2O_3, form : Cylindre, volume: 3 cm^3, Pt-Rh-Pt-thermocouple, sample atmosphere:: N_2, 5 l/min
Furnace:	medium temperature, heating rate: 10 °C/min, isothermic at 120 °C until no weight loss is observed (moisture), isothermic at 300 °C, isothermic at 600 °C, isothermic at 900 °C, isothermic at 1200 °C (identical with maximum temperature)

II X-Ray Diffractometry

Apparatus:	Philips Diffractometer
Excitation:	Cu tube, 30 kV 40 mA
Slits:	1° / 0.1 mm / 1°

For technical data of single crystal diffractometry see STERN (1977)

III Infrared Spectrometry

Apparatus:	IR-spectrophotometer Beckmann 4230
Source:	Nernst filament
Sample:	muscovite crystal with an uniform thickness of approx. 0.240 mm, beam perpendicular to (001)
Registration speed:	300 cm/min, gain: 1.3, period: 1 s, slit-width: 0.3 mm at 300 cm^{-1}

IV a X-Ray Fluorescence, Wavelength Dispersive

Apparatus:	Philips single channel vacuum spectrometer	
Excitation:	Ag tube, 40–50 kV, 30–60 mA	
Crystals:	graphite, Tl A P	
Integrations:	Si, Fe, Mn, Ca, Ti, K	10 s each
	Al	20
	Mg, P	40
	Na	100
Counter:	flow counter, pulse height discrimination	
Sample:	150 mg dried, ignited sample mixed with dried Merck $Li_2B_4O_7$ (2350 mg) melted to glass beads in Pt-Au crucibles subsequently in a muffle oven, and in a inductive furnace (STERN, 1979)	

IV b X-Ray Fluorescence, Energy Dispersive

Apparatus:	Tracor TN - 1710
Excitation:	Ag tube, 20–40 kV, 0.05 mA, ± primary Zn-filter
Integration:	200 s, peak stripping using «XML», software by Tracor
Sample:	direct excitation of cleaned mica surface, ~ 3 cm^2

Manuscript received March 5, 1982